Flux density monitoring at VGOS frequencies with the Onsala Twin Telescopes

Flux density monitoring at VGOS frequencies with the Onsala Twin Telescopes

A. Kinman, R. Haas, K. le Bail, J. Yang, E. Varenius

Abstract An accurate flux density catalog at the frequencies observed by the VLBI Global Observing System (VGOS) is needed to improve the scheduling of geodetic experiments. We present the setup and results of flux monitoring experiments performed with the Onsala Twin Telescopes (OTT) on a rather regular basis since June 2021. We have obtained time series of flux density in the standard bands that are used sofar for the VGOS Operational (VO) sessions, i.e. 3.0–3.5 GHz, 5.2–5.7 GHz, 6.3–6.8 GHz and 10.2–10.7 GHz. The experiments targeted approximately 200 ICRF3 defining sources that are visible from Onsala. In addition to these dedicated flux monitoring experiments with the OTT, we also analyzed OTT data from several VO sessions. All data were analyzed using Common Astronomy Software Applications (CASA). Due to local radio frequency interference at Onsala, few radio sources have reliable flux density values in the lowest VO-band (3.0—3.5 GHz). Most sources are found to be variable over time. We estimate a systematic uncertainty of 5 % and a statistical uncertainty of on average 1 % for our flux density results. In the future, we are interested in expanding the sample size, increasing baseline sensitivity and running collaboration observations with other facilities.

Keywords flux density, VGOS, geodetic VLBI, active galactic nuclei

Alva Kinman[1] · Rüdiger Haas[1] · Karine le Bail[1] · Jun Yang[1] · Eskil Varenius[2]
(1) Chalmers University of Technology, Onsala Space Observatory, Observatorievägen 90, Onsala, 439 92 Sweden
(2) on leave from Chalmers University of Technology, Onsala Space Observatory, Observatorievägen 90, Onsala, 439 92 Sweden

1 Introduction

The VLBI Global Observing System (VGOS) has been operational since 2020. With small, fast antennas and a large bandwidth, VGOS aims to improve the accuracy of geodetic parameters compared to the legacy system. The goal is to provide a station position accuracy of 1 mm (Petrachenko et al., 2012).

Reaching this goal requires an increased number of scans per experiment. A large number of scans allows better estimates of tropospheric delays and increases the precision of geodetic parameters. To optimize the use of observing time, the flux densities of the radio sources need to be known. The scan duration can then be adapted to each source such that a sufficient, but not excessive, signal-to-noise ratio (SNR) is reached.

Schartner et al. (2025) recently explored a SNR-based scheduling approach for VGOS. Flux densities were firstly predicted by inter-/extrapolation based on flux catalogs at S- and X-bands, and secondly derived from correlation amplitudes of VGOS-Operations (VO) sessions. Though their scheduling method provided promising results by increasing the number of scans compared to standard VGOS scheduling, there were discrepancies between predicted and measured SNRs. This indicates that more accurate flux density models are still needed. In particular, flux densities for variable sources need to be updated regularly.

With the aim of providing accurate and up-to-date flux densities for International Celestial Reference System (ICRF3) sources, we have devised a flux monitoring program using the Onsala Twin Telescopes (OTT). The telescopes are used to measure the flux density of geodetic sources in the frequency bands currently used for VGOS operations, i.e. 3.0–3.5 GHz, 5.2–5.7 GHz, 6.3–6.8 GHz and 10.2–10.7 GHz. In this proceedings paper, we describe the program. Section 2 describes the experimental setup and data analysis. Section 3 presents a first look at the results, while Section 4 presents the conclusions and outlook.

2 Observations and data analysis

We have derived flux densities from measurements with the Onsala Twin Telescopes (OTT). The telescopes have a diameter of 13.2 m and are located 75 m apart at Onsala Space Observatory (OSO). Two types of experiments have been analyzed: 1) dedicated flux monitoring experiments scheduled and observed locally at OSO, and 2) VGOS-Operational (VO) sessions via the International VLBI Service for Geodesy and Astrometry (IVS, Nothnagel et al., 2017), available through the Crustal Dynamics Data Information Systems (CDDIS)[1] database.

The standard VGOS frequency setup used for the experiments consists of four bands centered at 3.2, 5.5, 6.5 and 10.4 GHz. Each band in turn contains eight 32 MHz sub-bands. For the complete setup, see e.g. Varenius et al. (2022).

2.1 Flux monitoring experiments

The first flux monitoring experiments were scheduled in 2021 and involved only seven geodetic sources. These experiments are described in Varenius et al. (2022). The second round of flux monitoring experiments were observed starting in January 2023, and the results reported in this paper extend to April 2025. The experiments were scheduled using the software VieSched++ (Schartner & Böhm, 2019). The experiments initially had a duration of 20 hours and targeted all the defining sources that are visible from Onsala. This resulted in approximately 200 observed sources per experiment. In addition, the three flux calibrators 3C147, 3C286 and 3C295 were observed. Each source was observed in three scans, each with a duration of one minute.

After analysis of the first one and a half years of experiments, it was determined that the weaker sources needed longer scan durations in order for their fluxes to be measured reliably. From November 2024, the weaker sources were observed with a scan duration of two minutes. The same change was applied for the flux calibrators. To accommodate the extra observing time without decreasing the number of sources, the experiment duration was increased to 26 hours.

The experiments were scheduled approximately once a month. Longer gaps in the time series exist due to technical issues with the telescopes and lack of available storage space.

As of April 2025, 21 full-length (20–26 h) flux-monitoring experiments have been performed and analyzed, in addition to 49 of the short experiments presented in Varenius et al. (2022).

2.2 VGOS-operational experiments

Several VGOS-operational (VO) experiments have been analysed as well. Currently, the following VO sessions have contributed to the flux density catalog: vo3299, vo4108, vo4115, vo4248, vo4269, vo4311, vo4339, vo4346, vo5029, vo5043. To obtain accurate fluxes, a flux calibration scan is needed. Such scans are now regularly added locally at Onsala to the end of each VO session. The calibration scans consist of 120 seconds observation of at least one of the calibrator sources used for the flux monitoring experiments.

Correlated VO data for the OTT baseline was obtained from CDDIS. The number of scans and the scan duration both differ between sources. Not all sources observed in VO sessions are defining sources of ICRF3, which means that our catalog is extended by the addition of the VO sources.

2.3 Correlation and calibration

The flux monitoring experiments were correlated at OSO using the software correlator DiFX (Deller et al., 2007). The OTT record orthogonal linear polarizations, here denoted X and Y, and all four correlation products XX, XY, YX and YY were produced. The experiments were then processed using the software Common Astronomy Software Applications (CASA, The CASA Team et al., 2022) together with VLBI tools developed by JIVE[2]. The correlated data were converted from DiFX format to FITSIDI format. Then, the *append_tsys* tool was used to import system temperature values from

[1] https://cddis.nasa.gov/archive/vlbi/ivsdata/swin/

[2] https://github.com/jive-vlbi/casa-vlbi

the experiment into the FITSIDI file. The system temperature values were read from the experiment log and converted to antab file format. This antab file also included a fixed gain for each telescope.

In CASA, a pipeline was created to flag outliers and perform the necessary calibration steps. The CASA pipeline is a development of the pipeline used by Varenius et al. (2022). The first step was to remove the phase calibration signal. Since the phase calibration systems of the OTT are fed by the same hydrogen maser, the signals are highly correlated and visible as spikes in the cross-correlation data. We also removed the edge channels of each sub-band, to avoid impact from edge-channel noise on the subsequent bandpass normalization. After that, amplitude calibration was performed using system temperature and gain values. Furthermore, autocorrelation-corrections, fringe fitting and bandpass calibration was performed. In the flux monitoring experiments, bandpass and fringe fitting solutions were calculated from the first scan of 3C286 and then applied to the whole data set. In the VO experiments, OJ287 or 0059+581 were used instead. Additionally, the task *rflag* was used to remove outliers caused by unwanted electromagnetic radiation (UER).

After all calibration steps were performed, the data was averaged over time and channel within each sub-band. The amplitudes of the XX, XY, YX and YY correlation products were then averaged over all scans of the same source. A pseudo-Stokes I value was calculated:

$$I = \frac{XX + YY}{2}. \quad (1)$$

Note that no parallactic angle correction was performed due to the short baseline.

2.4 *Absolute flux density calibration*

As a final step we performed additional flux density calibration based on the three flux calibration sources. The expected flux density of each calibration source at each sub-band was obtained from the flux models presented in Perley & Butler (2017). The expected flux density was divided by the measured flux density to obtain a scale factor. The average scale factor among the three calibration sources was calculated and used to correct the flux density of all sources. The scale factor was calculated separately for each experiment, to account for instrumental variation over time. The scale factor also corrects systematic gain differences between sub-bands, as seen in Figure 1.

2.5 *Filtering and averaging*

Due to the short baseline, the data contains strong UER. While some of the affected data can be removed in the calibration stage, broadband interfering signals remain. The 3.2 GHz band is particularly affected. To mitigate this, the data was filtered based on cross-polarization. The cross-polarization products, XY and YX, are expected to be close to zero since most geodetic sources are unpolarized. If they are too large, this indicates the presence of polarized UER. Thus, sub-bands that had a XY or YX polarization of more than 15 % of the XX or YY polarization were discarded. The limit of 15 % was chosen empirically (in accordance with Varenius et al., 2022) to get robust results.

Finally, the sub-bands making up each VGOS band were averaged together. As an additional outlier filtration step, any sub-band that deviated more than a factor 2 from the median in the band was also discarded.

3 Results

We have obtained light curves with at least five epochs for 212 sources. A few selected light curves are presented in Figure 2. The plot shows flux density in all available VGOS bands as a function of time. The triangular markers represent dedicated flux monitoring experiments, while the outlined circles represent VO sessions. The flux measurements from VO sessions generally agree with the dedicated flux monitoring measurements for sources where both are available. This indicates that geodetic sessions can be used as a complement to dedicated flux monitoring sessions.

We note a rich variety of behavior among the sources. While source 0312+100 is stable during the measurement period, the other sources in Figure 2 vary significantly in flux over time. There is also spectral variation among the sources. The spectrum of a synchrotron source is typically proportional to $\nu^{-\alpha}$, where ν is the frequency and α the spectral index. The sample contains sources with both positive and negative spectral index. There are also examples of sources changing spectral index over time, seen in the

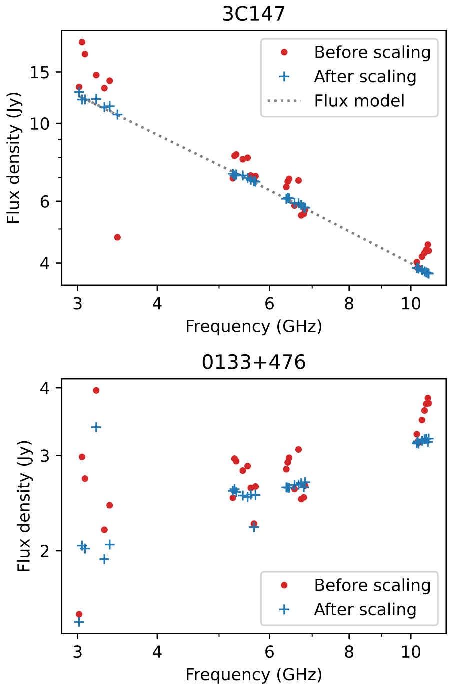

Fig. 1 The figure shows the effect of the scale factor in reducing systematic errors between sub-bands, exemplified by experiment fm5087. Top: 3C147, one of the flux calibrators used to determine scale factors. The dashed line shows the flux model from Perley & Butler (2017). Bottom: 0133+476, a bright source which was not used for calibration. The scaling clearly reduces the flux density scatter within each VGOS band.

bottom left of Figure 2. The complete flux catalog will be made available in a later publication.

We note that the majority of the sources are variable, which highlights the need for a continuously updated flux catalog. By comparing the lowest to the highest recorded flux in Band 4 (including only the sources that have at least five data points), we find that 82 % have varied by more than 20 % during the monitoring period. Furthermore, 39 % of sources have varied by more than 50 %.

As mentioned in Section 2.5, the 3.2 GHz band is heavily affected by UER. The cross-polarization filter criterion removes most of the data points in this band, leading to only a small subset of sources having a light curve at 3.2 GHz.

The error bars shown in Figure 2 were obtained in two steps. The standard error of the flux density in each band was obtained as the standard deviation of the included sub-bands divided by $\sqrt{N}$, where N is the number of sub-bands. On average, the standard error corresponds to 1 % of the flux density. Since these error bars fail to account for systematic errors such as gain curve uncertainty and UER, an additional 5 % error was added in quadrature.

To verify that the errors are reasonable, we calculated the reduced χ^2 value for a few sources which appear stable over time, similarly to Varenius et al. (2022). If the flux density of these sources is modeled as being constant in time, the reduced χ^2 value is below 1 for all bands (see Table 1). The size of the error thus appears to be reasonable or slightly overestimated.

Table 1 Reduced χ^2 values for stable non-calibrator sources

Source	Band 1	Band 2	Band 3	Band 4
0312+100	0.08	0.18	0.23	0.11
0552+398	0.19	0.62	0.22	0.60
M84	0.17	0.90	0.86	-

4 Conclusions and outlook

We have obtained light curves at the current operationally used VGOS frequencies for 212 geodetic sources. We plan to publish the dataset in its entirety in the near future. The monitoring is planned to continue with one experiment per month. In addition to flux monitoring experiments, we have also demonstrated the possibility of using data from geodetic experiments to calculate precise flux densities.

The produced flux catalog could be used to improve VGOS scheduling by optimizing the integration time such that the SNR goals are reached. The data could also be of interest for astronomy. The light curves allow tracking of source flux density and spectral index over time, which could provide valuable insights into the physical properties of the studied active galactic nuclei (e.g. Singh et al. 2020).

In order to use this data for VGOS scheduling, flux models for longer baselines are needed. There is also a need to expand the monitored source catalog to eventually cover all sources that are routinely observed by VGOS. Thus, more telescopes need to be involved. As a first step, observations with other twin telescopes would be beneficial to increase the number of sources and densify the light curves.

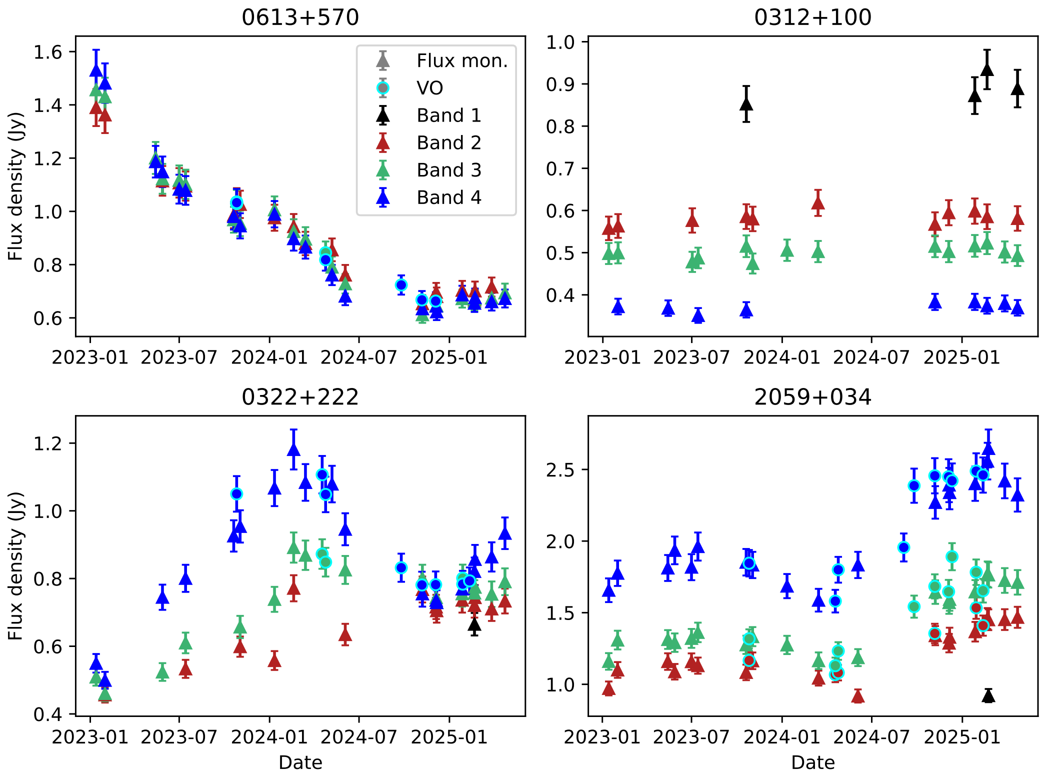

Fig. 2 Example light curves from the flux monitoring program. Triangles represent results from dedicated flux monitoring experiments and circles from VO experiments. The four colors represent VGOS band 1 (3.2 GHz), 2 (5.5 GHz), 3 (6.6 GHz) and 4 (10.4 GHz). The flux density of 0312+100 (top right) is relatively stable over the measurement period, while the other shown sources are more variable. Note the differences in spectral index, both between sources (compare 0613+570, 0312+100 and 2059+034) and between observations of the same source (compare 0322+222 in early 2024 and early 2025).

References

The CASA team, Bean, B., Bhatnagar, S. (2022) CASA, the Common Astronomy Software Applications for Radio Astronomy *Publications of the Astronomical Society of the Pacific*, Vol 134, 1041 doi: 10.1088/1538-3873/ac9642

Deller, A. T., Tingay, S. J., Bailes, M., West, C (2007) DiFX: A Software Correlator for Very Long Baseline Interferometry Using Multiprocessor Computing Environments. *Publications of the Astronomical Society of the Pacific*, Vol 119, 853, pp. 318-336 doi: 10.1086/513572

Nothnagel, A., Artz, T., Behrend, D., Malkin, Z. (2017) International VLBI Service for Geodesy and Astrometry – Delivering high-quality products and embarking on observations of the next generation. *Journal of Geodesy*, Vol. 91(7), pp. 711–721 doi: DOI 10.1007/s00190-016-0950-5

Perley, R. A., Butler, B. J. (2017) An Accurate Flux Density Scale from 50 MHz to 50 GHz. *The Astrophysical Journal Supplement Series*, 230, 1, id. 7 doi: 10.3847/1538-4365/aa6df9.

Petrachenko, W.T., Niell, A.E., Corey, B.E., (2012) VLBI2010: Next Generation VLBI System for Geodesy and Astrometry. *Geodesy for Planet Earth. International Association of Geodesy Symposia*, 136 doi: 10.1007/978-3-642-20338-1_125.

Schartner, M., Böhm, J. (2019) VieSched++: A New VLBI Scheduling Software for Geodesy and Astrometry *Publications of the Astronomical Society of the Pacific*, 131, 102, pp. 084501, doi: 10.1088/1538-3873/ab1820.

Schartner, M., Petrachenko, B., Titus, M. et al. (2025) Optimizing VGOS observations using an SNR-based scheduling approach. *Earth Planets Space*, 1, 77, 61, doi: 10.1186/s40623-025-02158-0.

Singh, K. K., Meintjes, P. J. (2020) Characterization of variability in blazar light curves. *Astronomische Nachrichten*, Vol. 341, 713, pp. 713-725 doi: 10.1002/asna.202013731

Varenius, E., Maio, F., Le Bail, K., Haas, R. (2022) Broad band flux-density monitoring of radio sources with the Onsala twin telescopes. *Experimental Astronomy*, 54, 1, p. 137-155, doi: 10.1007/s10686-022-09867-4.